remote sensing

Article

Spatial and Temporal Characteristics of Drought Events in Southwest China over the Past 120 Years

Ying Wang [1], Yuanmou Wang [2], Yanan Chen [1], Huan Chen [2], Xingting Li [1], Zhi Ding [1], Xujun Han [1] and Xuguang Tang [1,*]

[1] Chongqing Engineering Research Center for Remote Sensing Big Data Application, School of Geographical Sciences, Southwest University, Chongqing 400715, China; wy201105@email.swu.edu.cn (Y.W.); chenyanan@email.swu.edu.cn (Y.C.); lxt0008@email.swu.edu.cn (X.L.); dingzhi11@mails.ucas.ac.cn (Z.D.); hanxujun@swu.edu.cn (X.H.)

[2] China Meteorological Administration Economic Transformation of Climate Resources Key Laboratory, Chongqing Meteorological Service Centre, Chongqing 401147, China; njuwym9327@163.com (Y.W.); ricekkk0601@163.com (H.C.)

* Correspondence: xgtang@swu.edu.cn; Tel.: +86-23-68252370

Abstract: Global climate change, especially extreme drought events, presents a complicated challenge to humanity and Earth's system in the 21st century. As an extremely important carbon sink region in China, Southwest China has encountered frequent drought disasters in recent decades. It is critical to explore the frequency, duration, severity, and other associated characteristics of drought events as well as their spatial and temporal patterns in the region from a long-term perspective. In this study, we used the latest dataset from the Spanish National Research Council (CSIC) between 1901 and 2018 to extract all drought events by calculating the standardized anomaly of the Standardized Precipitation Evapotranspiration Index (SPEI). Theil–Sen median trend analysis, the Mann–Kendall test, and the moving *t*-test were used to reveal the spatial trend and mutation point of drought severity. The results showed that (1) The standardized anomaly of the 3-month SPEI can accurately identify drought events in Southwest China. In total, 72 drought events occurred during this period, of which the consecutive drought in autumn, winter, and spring from 2009 to 2010 lasted the longest, having the most substantial severity and the most extensive damage range. (2) Drought events mainly started in spring and early summer and ended in autumn and winter. The distribution of drought was the most expansive and the drought severity was the most serious in September. (3) In terms of spatial pattern, Guangxi has the highest frequency of drought events, with some areas experiencing up to 100 events. The average duration of drought events ranged between 3.5 and 5.5 months, with most lasting for 4–5 months. The most severe drought areas are mainly concentrated in southern Sichuan and western Yunnan. Overall, the severity of drought events in the west were generally higher compared to that in the east. (4) Over the past 120 years, most of the region (82.46%) showed an increasing trend in drought severity, with a slope of up to −0.01. About 15.12% of the areas exhibited a significant drying trend ($p < 0.05$), particularly in southern Sichuan, eastern Guizhou, and northern and southern Yunnan. Such analyses can serve as a scientific foundation for developing drought prevention and mitigation measures as well as exploring how drought events affect the structure and function of terrestrial ecosystems in Southwest China.

Keywords: drought event; spatiotemporal change; SPEI; Southwest China

check for updates

Citation: Wang, Y.; Wang, Y.; Chen, Y.; Chen, H.; Li, X.; Ding, Z.; Han, X.; Tang, X. Spatial and Temporal Characteristics of Drought Events in Southwest China over the Past 120 Years. *Remote Sens.* **2023**, *15*, 3008. https://doi.org/10.3390/rs15123008

Academic Editor: Gabriel Senay

Received: 11 April 2023
Revised: 23 May 2023
Accepted: 6 June 2023
Published: 8 June 2023

1. Introduction

Climate change can lead to changes in vegetation productivity, which can affect the pattern, structure, and function of terrestrial ecosystems [1–4]. With the intensification of global climate change, high temperature, heavy rain, drought, and other extreme climate events occur frequently [5]. Among these events, droughts are the most destructive natural disaster, which immediately impact the water balance of specific area and have a direct effect on the natural environment of society and the sustainable development of the human economy [6–8] From 1980 to 2009, the mean yearly financial damage caused by global droughts was USD 17.33 billion. The amount escalated to USD 23.125 billion from 2010 to 2017, surpassing the costs of other meteorological calamities by a significant margin [9]. Recent studies suggested that extreme weather events such as droughts will intensify over the course of the century in the context of climate change [10–14]. Regarding this fact, drought monitoring and assessment has attracted attention from scientists and government institutions worldwide across various fields [6,15,16]. Therefore, the utilization of long-term time series data to evaluate the spatiotemporal characteristics of drought is of critical importance in reducing the impact of drought and effectively managing associated risks.

The sixth assessment report of the Intergovernmental Panel on Climate Change (IPCC) working group I has provided a precise definition of drought, which is characterized by lower than average humidity conditions leading to a shortage of water resources, causing harm to various natural and economic sectors [17]. The latest IPCC definition distinguishes four categories of drought: meteorological drought, agricultural (soil moisture) drought, hydrological drought, and socioeconomic drought. Meteorological drought is the most commonly occurring type of drought and frequently serves as a precursor to other forms of drought [18]. Currently, global and regional drought monitoring is generally carried out by employing the drought index [19]. How to choose an appropriate drought index serves as the foundation for monitoring regional drought conditions [20]. Three widely used drought indices include the Palmer Drought Severity Index (PDSI) [21], Standardized Precipitation Index (SPI) [22], and Standardized Precipitation Evapotranspiration Index (SPEI) [23]. SPEI was developed by incorporating potential evapotranspiration into the construction of the SPI index. Compared with the traditional indices, SPEI has unique advantages, making it a valuable tool for monitoring drought globally. By combining the strengths of PDSI and SPI, SPEI incorporates the impact of both temperature and precipitation on drought. It maintains PDSI's sensitivity to changes in evapotranspiration and offers the simplicity of SPI's calculation with the ability to analyze drought over multiple time scales. Therefore, SPEI is highly suitable for large-area monitoring the characteristics of drought events under the context of climate change [19,24].

Persistent severe droughts have afflicted large areas of China on various time scales in recent decades, with an escalation in both frequency and severity of such drought events [25,26]. Southwest China has been predicted to be the most drought-prone region under current and future climate scenarios, especially due to its extensive karst topography that makes it difficult to keep water in the soil [27–29]. At present, much research has been conducted on the temporal and spatial characteristics of drought in Southwest China using different analysis methods. For example, Li et al. [30] used SPEI to demonstrate a drying trend in Southwest China, with a noteworthy reduction in average values from 1980 to 2012, and indicated that SPEI outperformed SPI slightly. Based on data from 142 meteorological stations, Jia et al. [31] computed the daily SPEI for both annual and seasonal time scales and revealed that Southwest China experienced a rising trend in the regional average drought severity as well as all-drought. Tang et al. [32] combined meteorological and hydrological data with historical drought records and demonstrated that the occurrence of drought events rose in frequency in the 21st century. Notably, the southern region of Southwest China has been plagued by severe droughts. These findings have important implications for using SPEI to reveal the spatiotemporal features of drought evolution in Southwest China. However, since there were few meteorological stations in West China before 1950, most research focused on the post-1949 period. Thus, research has lacked extraction and analysis of historical drought events.

Therefore, on the basis of the SPEI dataset from 1901 to 2018, this study aimed (1) to capture all drought events in Southwest China over the past 120 years and quantitatively describe the severity, starting and ending months, and duration of each drought event; (2) to investigate the spatial patterns of drought events, including frequency, duration, and severity; and (3) to reveal the spatiotemporal trends of drought severity in the region as well as relevant significance level. These analyses will enhance our understanding of the evolution of drought characteristics in Southwest China, which is helpful for developing efficient drought prevention and mitigation strategies.

2. Data and Methods

2.1. Study Area

The study area, which encompasses approximately 1.37×10^6 km^2 of Southwest China extending from 20°54′N to 34°19′N and from 96°21′E to 112°04′E, is composed of five provinces, namely, Sichuan, Yunnan, Guizhou, Guangxi, and Chongqing (Figure 1). With diverse terrain and topographical disparities, the area borders the Qinghai–Tibet Plateau to the west, the Sichuan Basin to the east, and the Yunnan–Guizhou Plateau to the south [33]. The region has a subtropical monsoon climate, which is characterized by annual mean temperature between 14 °C and 24 °C and total precipitation between 600 mm and 2300 mm. The natural rainfall exhibits a decreasing spatial trend from southeast to northwest, attributable to the influence of complicated topography. Moreover, the seasonal distribution is extremely uneven, with hot and humid summers and cold and dry winters, and 80–90% of precipitation occurring in May–October and 10%–20% in November–April [34]. Recently, drought events occurred frequently in this region, which can be linked to the exacerbation of global climate change.

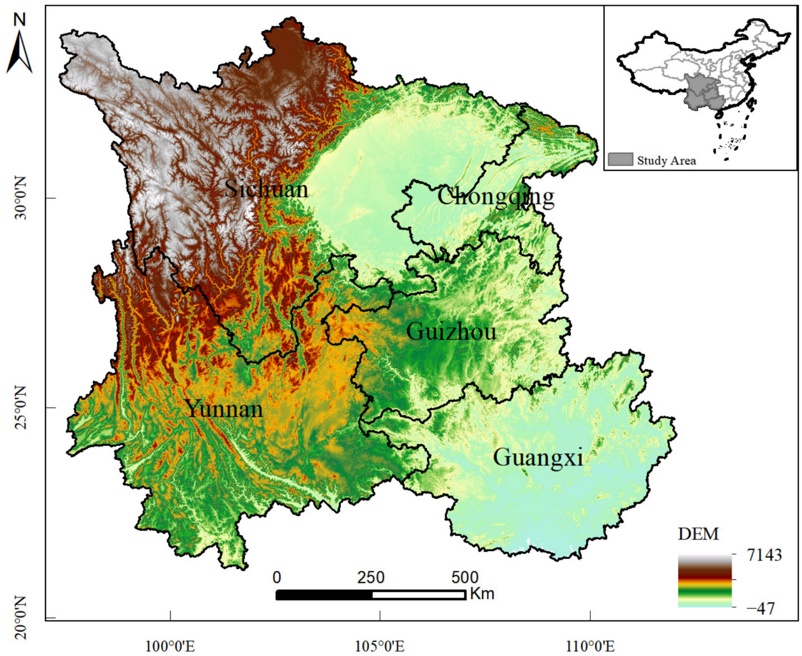

Figure 1. Location of the study area.

2.2. Data

The gridded SPEI dataset (SPEIbase v2.6) used is derived from the Spanish National Research Council (CSIC) (https://digital.csic.es/handle/10261/202305 (accessed on 8 October 2021)), covering the global continents (excluding Antarctica) spatially with a spatial resolution of 0.5° and ranging from 1901 to 2018. The SPEI dataset, which spans a time range of 1 to 48 months, displays the cumulative water surplus or deficit over the 1 to 48 months previous. It is therefore appropriate for describing different types of drought events. In this study, we utilized the 3-month SPEI (indicated as SPEI$_3$) to identify drought events. Such time scale has been demonstrated to be effective to characterize short-term fluctuations in soil moisture conditions [35,36]. Furthermore, Li et al. [37] have demonstrated that SPEI$_3$ can accurately depict the spatial and temporal distribution of seasonal drought events in Southwest China.

2.3. Methods

2.3.1. Identification of the Drought Event

This study employed the monthly $SPEI_3$ to detect the onset, end, duration, and severity of the drought events in Southwest China between 1901 and 2018. Furthermore, the standardized anomaly of $SPEI_3$ (SA_{SPEI_3}) was calculated for the specific month (tth month) within the drought period for each grid cell:

$$SA_{SPEI_3} = \frac{SPEI_3^{i,t} - \overline{SPEI_3^{i,t}}}{\delta\left(SPEI_3^{i,t}\right)}(t = 1, 2, \ldots, 12)$$

The nondimensional index SA_{SPEI_3} is used to uncover the standard deviation of $SPEI_3$ in a particular month from its mean value over several years during the reference period of 1901–2018. Here, $SPEI_3^{i,t}$ refers to the value of $SPEI_3$ for the ith grid in the tth month during a drought event, and $\overline{SPEI_3^{i,t}}$ denotes the average value of $SPEI_3$ for the ith grid in the tth month throughout the study period (1901–2018). The standard deviation (SD) of $SPEI_3$ for the ith image in the tth month over the reference period [37,38] is represented by $\delta\left(SPEI_3^{i,t}\right)$.

On this basis, the SA_{SPEI_3} was initially subjected to a 3-month moving window smoothing technique as proposed by Saft et al. [39]. Through this smoothing method, a long and continuous dry period can be avoided from being unreasonably interrupted by a single humid month. As a result, the smoothed SA_{SPEI_3} can accurately detect the beginning and end of drought occurrences. Figure 2 demonstrates how drought onset and end are identified using SA_{SPEI_3}. The first month with SA_{SPEI_3} below the -0.5 threshold (orange triangle) is considered to be the beginning of a drought, while the first month with SA_{SPEI_3} upcrossing the same threshold (inverted orange triangle) is considered to be the end of the drought. The selection of the threshold is in line with previous research [37].

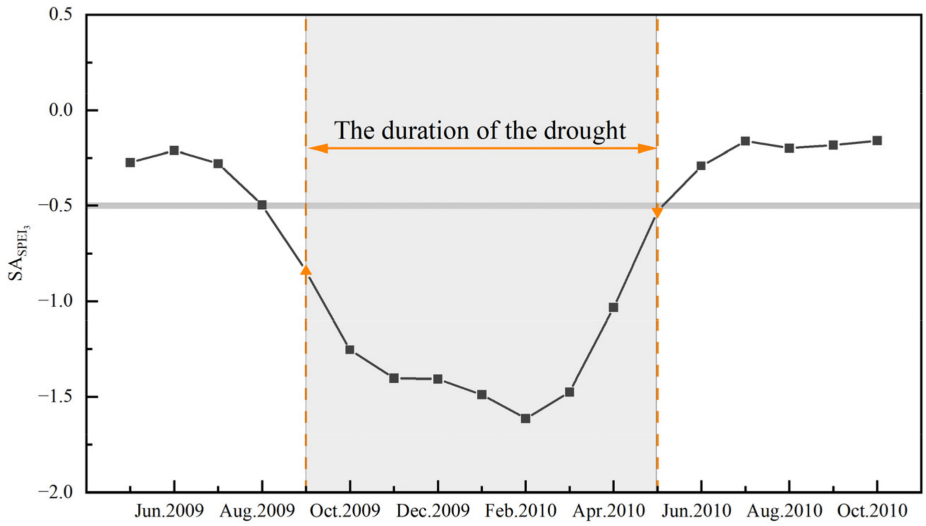

Figure 2. The schematic diagram for identifying drought characters. Here, we took the drought event that occurred in 2009–2010 as an example.

2.3.2. Characterization of Drought Events with Run Theory

Yevjevich's run theory [40] offered an effective approach to extract drought characteristics, including parameters such as duration, severity, and frequency to characterize each event. The part of the drought time series with values above or below the threshold is referred to as a "run", denoting a positive or negative run, respectively [41]. According to run theory, the drought frequency is the number of events (N) when the SA_{SPEI_3} is below the threshold level, and the drought duration is the period of time when the SA_{SPEI_3} is consistently below the threshold. The severity of drought event is determined by the mean of SA_{SPEI_3} multiplied by the duration of each drought event ($S = \overline{SA_{SPEI_3}} \times$ duration). This approach has been widely implemented in previous studies conducted across multiple regions worldwide [42–46].

2.3.3. Trend Analysis

This study used the Theil–Sen median slope estimation to calculate long-term trend in the severity of drought events in Southwest China between 1901 and 2018, followed by a Mann–Kendall (M–K) trend test [47] to determine the significance of the changing tendency. Compared to linear regression, Sen slope estimation is a nonparametric statistical trend analysis method. The method is computationally efficient and suitable for trend analysis of long-time series. The formula is as follows:

$$slope = Median\left(\frac{x_j - x_i}{j - i}\right)\forall j > i$$

where $Median()$ represents the median value; i, j are the number of time series; and x_i, x_j represent the severity value of the i, j time pixels, respectively. $slope > 0$ indicates an upward trend of the time series, representing a wetting trend; the opposite is an aggravating trend. The M–K test at the 0.05 level is set as significant.

2.3.4. Mutation Analysis

The moving t-test method was used to analyze the mutation of the intensity of all drought events and identify the mutation point. The significance level of α = 0.05 was selected to obtain the critical value according to the t-distribution table. When $T > |t_\alpha|$, then the two series before and after the moving point are significantly different.

3. Results

3.1. Temporal Distribution of Drought Events

Figure 3 displays all drought events in Southwest China between 1901 and 2018 extracted by standardized anomaly of SPEI. On this basis, the onset, end, duration, and magnitude of each drought event were systematically evaluated, alongside the year in which they occurred (Table 1). Before the 1930s, there were fewer drought occurrences, and the overall situation was humid. By the 1930s, the number of droughts increased significantly, including a severe drought in 1936–1937 with an S value of -7.23, followed by a significant drought event in summer of 1939, which lasted until January of the following year. During the 1940s, several droughts occurred consecutively. In the 1950s and 1980s, the overall wet and dry distribution was relatively balanced, but more severe drought events occurred in 1962–1963, 1969, and 1987, with S values of -8.61, -7.28, and -5.51, respectively. In the early 1990s, droughts and floods were more frequent, and this area was overall wet. By the late 20th and early 21st centuries, Southwest China encountered a full-scale drought period. In particular, the autumn–winter–spring drought event that occurred in 2009–2010, with S values reaching up to -11.58, affected the entire region and was considered as the most severe drought in the last 120 years. Additionally, during the summer of 2011, another widespread megadrought happened, with S-values of -7.169. In general, during the past 120 years, Southwest China has had its worst drought conditions, including the 1930s and the early 21st century, with as many as nine drought events. During the remaining years, the region exhibited a relatively humid or balanced state between wet and dry, characterized by fewer drought events and lower severity.

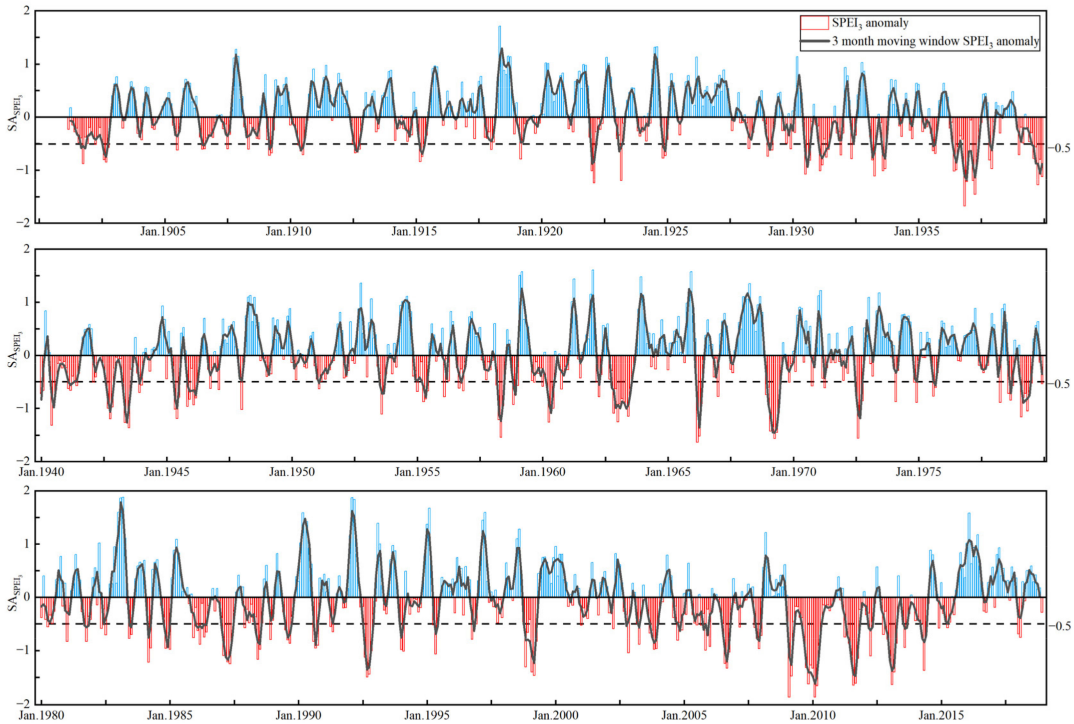

Figure 3. The temporal changes in the standardized anomaly of SPEI$_3$ in Southwest China between 1901 and 2018. The blue color and red color represent wet and dry periods, respectively.

Table 1. Statistics of drought events in Southwest China from 1901 to 2018. ID refers to the serial number of the drought event.

ID	Year	Start Time (Month)	End Time (Month)	Duration (Month)	*S* Value
1	1901	9	11	3	−1.7121
2	1902	8	9	2	−1.4338
3	1906	7	8	2	−1.0529
4	1909	3	4	2	−1.1518
5	1910	6	7	2	−1.19
6	1912	8	9	2	−1.2542
7	1915	3	5	3	−1.8304
8	1922	1	3	3	−2.2424
9	1923	2	3	2	−1.1955
10	1924	11	12	2	−1.1969
11	1929	2	2	1	−0.6134
12	1930	7	9	3	−2.2326
13	1931	2	6	5	−3.3202
14	1933	3	4	2	−1.4099
15	1933	8	9	2	−1.4713
16	1935	8	9	2	−1.061
17	1936	6	8	3	−2.1941
18	1936–1937	10	5	8	−7.2346
19	1937	11	12	2	−1.1268
20	1939–1940	7	1	7	−5.5929
21	1940	6	8	3	−2.3216
22	1941	2	4	3	−1.5879
23	1942	8	11	4	−3.2974
24	1943	4	8	5	−4.3866
25	1943	12	12	1	−0.5333
26	1945	5	7	3	−2.3208
27	1945–1946	11	3	5	−3.3344

Table 1. *Cont.*

ID	Year	Start Time (Month)	End Time (Month)	Duration (Month)	S Value
28	1951	2	2	1	−0.5272
29	1953	7	9	3	−1.986
30	1955	4	5	2	−1.324
31	1956	10	10	1	−0.517
32	1958	4	6	3	−3.2344
33	1958	11	12	2	−1.3555
34	1960	3	6	4	−3.2463
35	1962	4	4	1	−0.554
36	1962–1963	10	7	10	−8.6077
37	1966	3	5	3	−3.1387
38	1969	1	6	6	−7.284
39	1972	7	9	3	−3.0389
40	1975	9	9	1	−0.5691
41	1978	9	9	1	−0.7142
42	1979	2	6	5	−3.9129
43	1981	9	11	3	−1.6323
44	1982	6	6	1	−0.5065
45	1983	6	7	2	−1.09676
46	1984	3	4	2	−1.316
47	1984	11	12	2	−1.6816
48	1986	1	6	6	−3.2545
49	1987	1	6	6	−5.5077
50	1988	5	7	3	−2.3874
51	1989	7	9	3	−2.0077
52	1990	9	9	1	−0.8976
53	1992	8	11	4	−4.5228
54	1994	1	2	2	−1.267
55	1995	5	6	2	−1.2403
56	1996	11	11	1	−0.6344
57	1998–1999	11	4	6	−5.377
58	2002	10	10	1	−0.5428
59	2003	4	4	1	−0.5691
60	2003	9	12	4	−2.9458
61	2004	11	11	1	−0.6352
62	2005	10	12	3	−1.8395
63	2006	7	10	4	−3.7594
64	2007	11	12	2	−1.5976
65	2009	2	4	3	−3.0694
66	2009–2010	8	5	10	−11.5806
67	2011	5	11	7	−7.169
68	2012	3	5	3	−1.7632
69	2012–2013	11	4	6	−5.7842
70	2013	8	9	2	−1.1728
71	2014	4	6	3	−2.3386
72	2015	4	4	1	−0.5032

3.2. Spatial Pattern of Drought Characteristics

The frequency, average duration, and average S value of drought events occurring in each pixel were extracted by calculating SA_{SPEI_3} per pixel, as illustrated in Figure 4. The results showed that Guangxi Province has the highest frequency of drought, with some areas experiencing up to 100 events, followed by the northeast and southwest parts of Chongqing, while the central and southeast regions of Yunnan also exhibited high frequencies of droughts, with more than 85 events. The number of drought events in western Sichuan and Yunnan was less than 80. The mean duration of droughts ranged between 3.5 and 5.5 months, with most lasting for 4–5 months and a few, such as in northern and western Yunnan, lasting over five months. The averaged S value of drought events, calculated by summing the S values of all droughts in each pixel and dividing by the number of events, provided an estimation of the severity of each drought. Southern Sichuan typically has worse drought conditions, with the S value dropping below -5.1. Overall, the S values of drought events differed significantly from east to west, with the S value in the west being generally higher than that in the east.

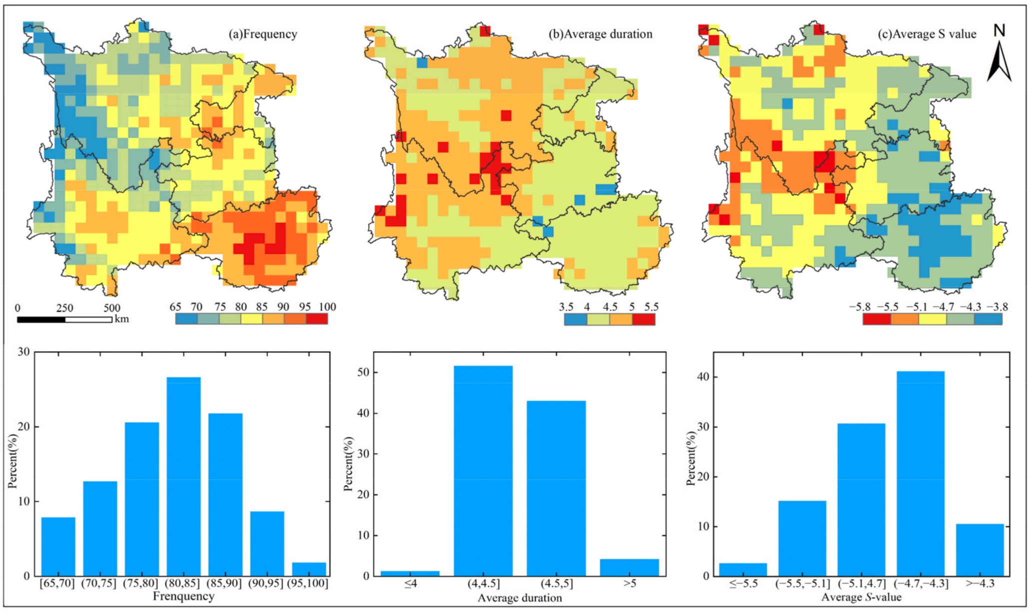

Figure 4. Frequency, average duration, and average S value of drought events in Southwest China.

Figures 5 and 6 presented the spatial and temporal distribution of drought events, including the onset and end times in Southwest China, respectively. Overall, the onset of drought mainly occurred in March, June, and August and was primarily concentrated in spring and summer, with rare occurrences in January and October. In regard to the end time, these drought events mainly finished in December and January, followed by April and October, and rarely ended in summertime. From a regional perspective, the Chongqing area is prone to high-temperature droughts, with drought events primarily starting in March, April, and June and typically ending in September. Droughts in Sichuan Province primarily occurred in late spring and early summer, with the end time being mainly in April or October. The start time of drought in Guizhou Province was not stable, with droughts happening in some regions during every season. However, the end time of drought in Guizhou Province was similar to that in Chongqing. Drought in Guangxi mainly started in spring and summer, with the highest frequency in March, and ended in autumn and winter, especially in September, December, and January. In Yunnan Province, droughts occurred mainly in June and September, with the end time similar to Guangxi, primarily in the autumn and winter.

Figure 7 provides the statistics on the severity of drought events occurring during different months. The analysis revealed that the most severe droughts mainly appeared in autumn, with September as the peak month, followed by summer, while winter exhibited the mildest drought condition, especially in January and February. The center of gravity of drought severity in spring shifted from northwest to southeast, with more severe droughts in central Sichuan during March and April and in Guangxi during May. The severe summer drought happened across a large part of southwestern China, especially in Chongqing and central Yunnan. In autumn, the most severe droughts occurred in September, affecting eastern Sichuan, southern Chongqing, and east and central Yunnan. However, the drought severity reduced in October and November, with eastern Guizhou, western Guangxi, and northwestern Sichuan exhibiting noticeable improvement. In winter, drought conditions were not severe except for December, and areas in Guizhou, eastern Guangxi, and southern Yunnan were relatively serious.

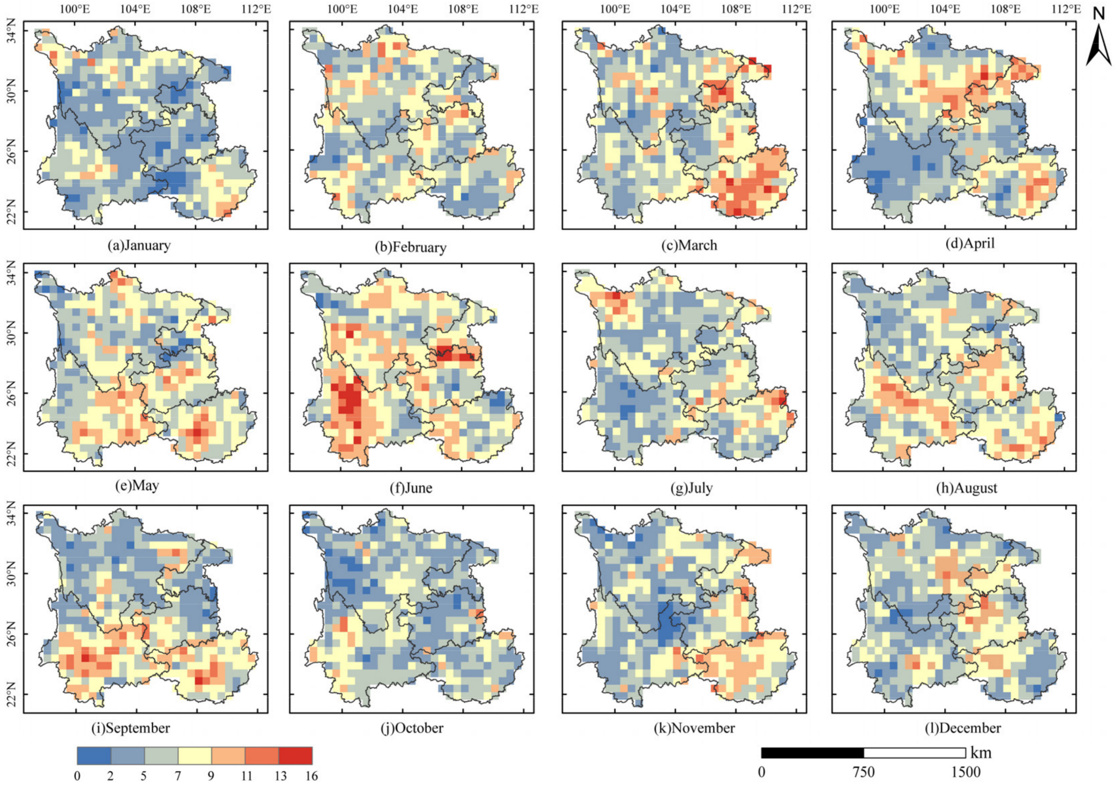

Figure 5. Frequency of drought events in different starting months in Southwest China.

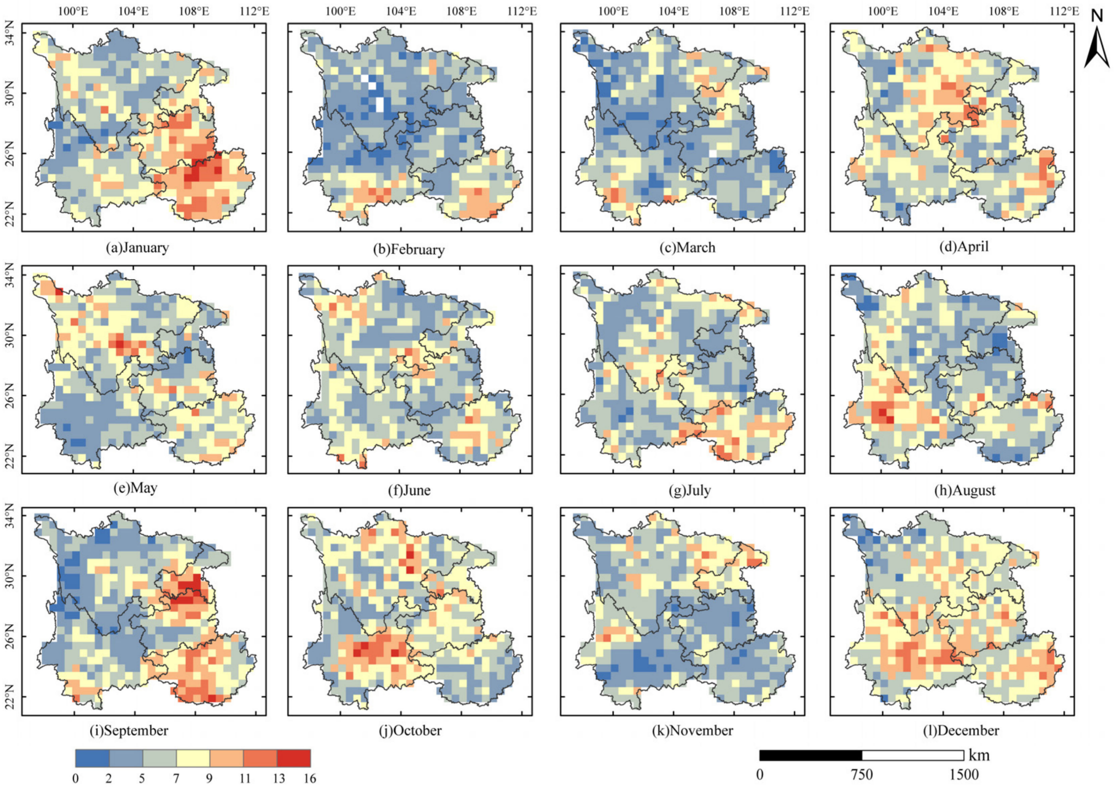

Figure 6. Frequency of drought events in different ending months in Southwest China.

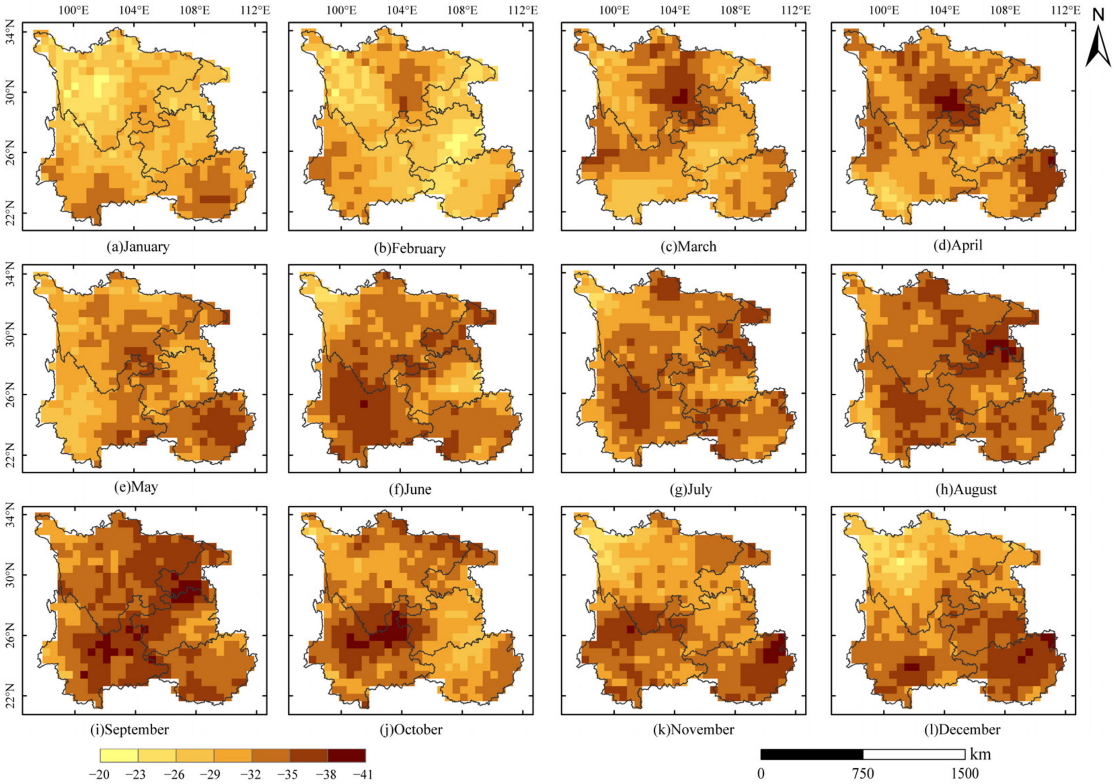

Figure 7. The severity of drought events in different months in Southwest China.

3.3. Trend of Drought Events

3.3.1. Overall Interannual Trend

Figure 8 shows a decreasing trend in the *S* values of drought events in Southwest China between 1901 and 2018, with the slope of −0.019, indicating an overall tendency of drought aggravation. However, the significance level of such trend did not pass $p < 0.05$. The *S* values of drought events throughout the past 120 years were then analyzed for mutation using a moving *t*-test, as shown in Figure 9, with the ordinal numbers corresponding to each drought event in order. The study revealed a distinct mutation point at ordinal number 24, which corresponded to the aggravation of drought in 1943. Further analysis indicated that the mean *S* value of drought events before 1943 was −2.17, while the mean *S* value after 1943 was −2.60, implying an apparent rise in the intensity as well as the frequency of drought in Southwest China.

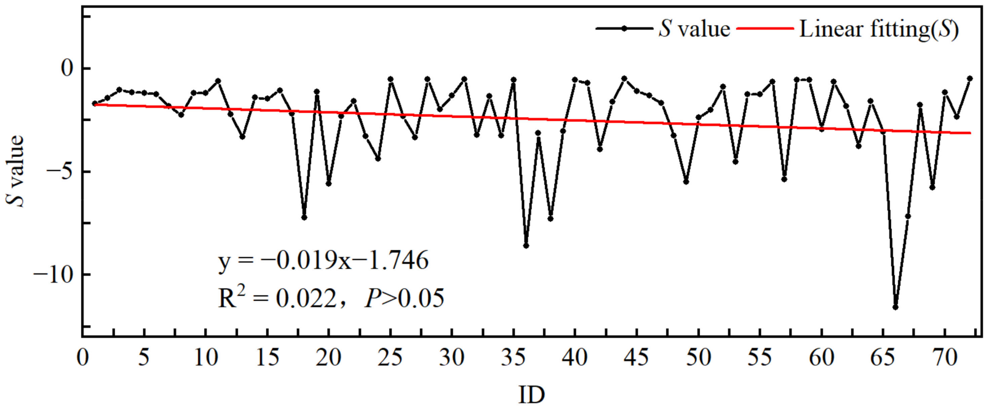

Figure 8. Variation trend of *S* value of drought events in Southwest China from 1901 to 2018. ID refers to the serial number of the drought event.

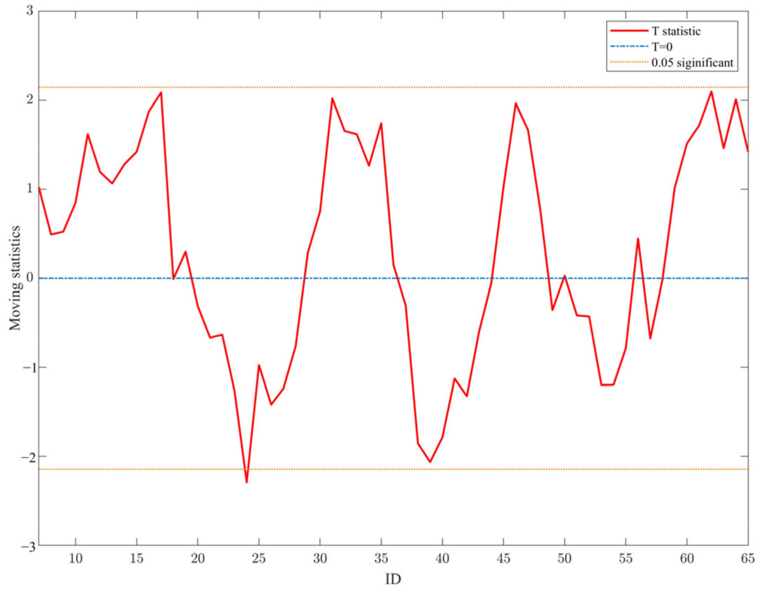

Figure 9. Moving *t*-test of *S* value of drought events in Southwest China from 1901 to 2018. ID refers to the serial number of the drought event.

3.3.2. Spatial Trend Analysis

Figure 10 showed the spatial distribution of droughts in Southwest China between 1901 and 2018. The coefficient β ranged from −0.071 to 0.036. According to statistics, the proportion of areas with a downward trend (82.46%) was far more than that of those with an upward trend (17.54%). The entire region was dominated by a distinct aridity trend. Notably, strong spatial differences were observed in the magnitude of the decline, with 15.12% of the areas exhibiting a significant decreasing trend ($p < 0.05$), particularly in southern Sichuan, eastern Guizhou, and northern and southern Yunnan. The coefficient of aridity trend in some regions even exceeded −0.04. Conversely, the wetting trend was predominantly observed in northern Sichuan, western Chongqing, and northeastern Guangxi.

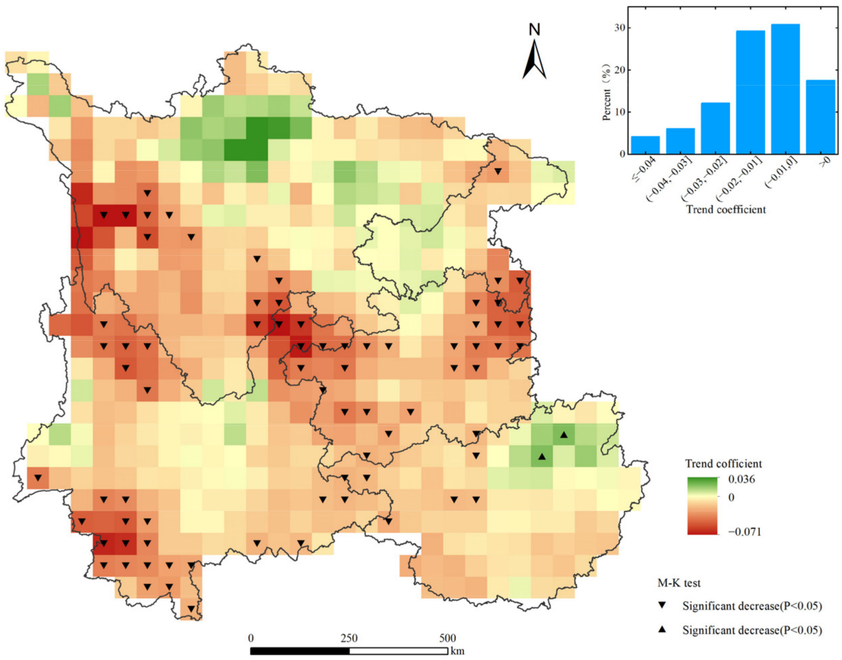

Figure 10. Spatial trend analysis of the *S* value of drought events in Southwest China from 1901 to 2018.

4. Discussion

In recent years, it has been a hot issue to examine the drought frequency, duration, and intensity with various indicators across different spatial scales [48–50]. Due to the complexity of drought and its widespread effects, it is necessary to select appropriate drought indices and time scales [51]. Through systematic analysis, this study extracted the drought events between 1901 and 2018 using the SA_{SPEI_3} method, which normalized the original values by scaling them based on the mean and unit variance, as this method has been shown to be effective in capturing drought events [37,38,52,53]. Previous research by Li et al. [54] detected 87 instances of regional drought events using the OITREE method and reported a marked rise in the frequency and intensity of drought during 1960–2010, while Wang et al. [55] extracted 87 drought events based on $SPEI_3$ from 1901 to 2009. Nevertheless, the results of our study differed from previous studies due to differences in the research periods and definitions of droughts. Notably, compared to other methods, the smoothed $SPEI_3$ anomalies were able to clearly identify the onset and end of drought events and have good applicability in Southwest China. Based on the S values of such drought events, the most severe droughts occurred in 1937, 1962–1963, 1969, 2009–2010, and the summer of 2011, which has been confirmed by previous research [56–61]. The most severe extreme drought event in the past 120 years took place during 2009/2010, which led to a significant decrease in vegetation productivity and a serious shortage of drinking water for 8.1 million people [60,62], threatening the security of the regional ecosystems [33,63]. Cui et al. [64] indicated that the primary factor in the 2009–2010 drought was the anomalous circulation, with more powerful than usual subtropical high pressure in the Western Pacific, leading to less precipitation in the region [65]. Sun et al. [58] also showed that the impact of evapotranspiration was comparable and even more prominent than that of precipitation.

In addition, there is considerable spatial variability in the frequency, duration, and severity of extreme drought events in Southwest China (Figure 4). Guangxi Province suffered from high-frequency but weak-severity droughts, while south Sichuan and northwest Yunnan experienced long-term, strong-severity but low-frequency droughts [60]. With regard to the occurrence time of the severe drought events, this study found that droughts in autumn were the most severe, followed by droughts in summer, which is consistent with Tang et al. [32] and Wang et al. [66]. Furthermore, much recent research has underscored the importance of identifying the beginning, end, and severity of droughts, as well as establishing early warning systems for monitoring them [24,48,67,68].

In Southwest China, there has been a noticeable increase in the incidence and extent of extreme droughts along with a warming–drying trend [38,69–72]. The study further suggests that this region has experienced the most significant increase in drought frequency since the beginning of the 21st century [32]. Spatially, there is strong spatial heterogeneity in drought severity and trends in Southwest China. During the period 1901–2018, southern Sichuan, eastern Guizhou, and northern and southern Yunnan exhibited significant drying trends, while a few areas such as northern Sichuan, western Chongqing, and northeastern Guangxi showed a wetting trend. This is mainly attributed to the decrease in precipitation and the associated increase in temperature [25,58]. In the context of a warming climate, the weakening of the Indian Ocean monsoon has reduced the availability of water vapor, which has led to a more severe drought trend in the region [73,74].

In our study, the SPEI was used for identifying drought events in the past 120 years in Southwest China. In fact, monitoring, assessing, and forecasting droughts posed significant challenges since no single method or index can accurately capture the diverse causes and wide spatiotemporal variations of all types of droughts [75]. There are more than 150 drought indices that are widely recognized as useful tools for monitoring drought events [20,76]. In addition to meteorological drought indices, soil moisture (SM) plays a crucial role in monitoring agricultural droughts during the plant growing season and is an effective means of evaluating crop yield losses resulting from climate shock [77–79]. Several agricultural drought indices take into account SM, such as the Soil Moisture Anomaly Index [80], Normalized Soil Moisture [81], Soil Moisture Index [82], and Soil Water Deficit

Index [83]. However, drought indices that are based on soil moisture tend to be more intricate than meteorological drought indices [79]. In addition, it can be challenging to obtain high-resolution drought information using these indices because remote sensing-based soil moisture measurements are frequently only accessible at a coarse spatial resolution [84]. Fortunately, Li et al. [85] introduced a long-term dataset of soil moisture with a resolution of 1 km, which was created using machine learning that had been trained on in situ observations from 1789 stations around China. This dataset can be utilized for numerous hydrological, meteorological, and ecological analyses and models.

5. Conclusions

This study detected the spatiotemporal patterns of drought characteristics in China's Southwest region over the last 120 years. We mainly found that drought events in this area can be well identified by calculating the SPEI. From 1901 to 2018, a total of 72 drought events of varying severity occurred in Southwest China. Among them, the most severe drought occurred from 2009 to 2010, which lasted from autumn, through winter, to the subsequent spring, with an S value of -11.58, covering almost the entirety of southwestern China. Since the beginning of the 21st century, drought conditions have been more intense and frequent. Meanwhile, Southwest China has been a region prone to drought events, with Guangxi experiencing the highest frequency, followed by Yunnan and Guizhou Provinces. Drought events were relatively less in the northern and western regions of Southwest China. The most severe droughts were concentrated in southern Sichuan and northern Yunnan. The duration of drought events typically lasted for about 3–5 months in this region. Droughts in Chongqing and Guangxi usually started in spring and early summer and ended in autumn. September has the widest distribution of aridification with the most severe drought event. Moreover, there is a general increasing trend of drought events between 1901 and 2018. Spatially, most of the regions, except for northern Sichuan and Guangxi, showed an increasing trend in drought severity, with a trend coefficient of up to -0.017. Such analyses can help us better understand the impact of global climate change on drought events in this region, provide scientific basis for investigating drought warnings and their ecological and environmental consequences, and formulate global policies and measures to effectively cope with droughts for sustainable development.

Author Contributions: Conceptualization, X.T.; methodology, Y.W. (Ying Wang), H.C. and X.L.; validation, Y.W. (Ying Wang), Y.C. and Z.D.; formal analysis, Y.W. (Yuanmou Wang), H.C. and X.L.; resources, X.H.; writing—original draft preparation, Y.W. (Ying Wang); writing—review and editing, X.T. and X.H.; funding acquisition, X.T. All authors have read and agreed to the published version of the manuscript.

Funding: This study was jointly supported by the National Major Projects on High-Resolution Earth Observation System (Grant No. 21-Y20B01-9001-19/22) and Chongqing Meteorological Department Business Technology Research Project (Grant No. YWJSGG-202310).

Data Availability Statement: All data can be accessed through the provided website.

Acknowledgments: We are grateful to the developers of SPEIbase v2.6 products provided by the Spanish National Research Council.

Conflicts of Interest: The authors declare no conflict of interest.

References

1. Richardson, A.D.; Hufkens, K.; Milliman, T.; Aubrecht, D.M.; Chen, M.; Gray, J.M.; Johnston, M.R.; Keenan, T.F.; Klosterman, S.T.; Kosmala, M.; et al. Tracking vegetation phenology across diverse North American biomes using PhenoCam imagery. *Sci. Data* **2018**, *5*, 180028. [CrossRef] [PubMed]
2. Tang, X.; Xiao, J.; Ma, M.; Yang, H.; Li, X.; Ding, Z.; Yu, P.; Zhang, Y.; Wu, C.; Huang, J.; et al. Satellite evidence for China's leading role in restoring vegetation productivity over global karst ecosystems. *For. Ecol. Manag.* **2022**, *507*, 120000. [CrossRef]
3. Li, G.; Wu, C.; Chen, Y.; Huang, C.; Zhao, Y.; Wang, Y.; Ma, M.; Ding, Z.; Yu, P.; Tang, X. Increasing temperature regulates the advance of peak photosynthesis timing in the boreal ecosystem. *Sci. Total Environ.* **2023**, *882*, 163587. [CrossRef] [PubMed]

4. Gong, H.; Cao, L.; Duan, Y.; Jiao, F.; Xu, X.; Zhang, M.; Wang, K.; Liu, H. Multiple effects of climate changes and human activities on NPP increase in the Three-north Shelter Forest Program area. *For. Ecol. Manag.* **2023**, *529*, 120732. [CrossRef]
5. Min, S.; Zhang, X.; Zwiers, F.W.; Hegerl, G.C. Human contribution to more-intense precipitation extremes. *Nature* **2011**, *470*, 378–381. [CrossRef] [PubMed]
6. Sur, K.; Lunagaria, M.M. Association between drought and agricultural productivity using remote sensing data: A case study of Gujarat state of India. *J. Water Clim. Chang.* **2020**, *11*, 189–202. [CrossRef]
7. Liu, X.; Zhu, X.; Pan, Y.; Zhao, A.; Li, Y. Spatiotemporal changes of cold surges in Inner Mongolia between 1960 and 2012. *J. Geogr. Sci.* **2015**, *25*, 259–273. [CrossRef]
8. Stocker, T. *Climate Change 2013: The Physical Science Basis: Working Group I Contribution to the Fifth Assessment Report of the Intergovernmental Panel on Climate Change*; Cambridge University Press: Cambridge, UK, 2014.
9. Su, B.; Huang, J.; Fischer, T.; Wang, Y.; Kundzewicz, Z.W.; Zhai, J.; Sun, H.; Wang, A.; Zeng, X.; Wang, G. Drought losses in China might double between the 1.5 °C and 2.0 °C warming. *Proc. Natl. Acad. Sci. USA* **2018**, *115*, 10600–10605. [CrossRef]
10. Zhang, R.; Wu, X.; Zhou, X.; Ren, B.; Zeng, J.; Wang, Q. Investigating the effect of improved drought events extraction method on spatiotemporal characteristics of drought. *Theor. Appl. Climatol.* **2022**, *147*, 395–408. [CrossRef]
11. Wang, Q.; Qi, J.; Qiu, H.; Li, J.; Cole, J.; Waldhoff, S.; Zhang, X. Pronounced Increases in Future Soil Erosion and Sediment Deposition as Influenced by Freeze-Thaw Cycles in the Upper Mississippi River Basin. *Environ. Sci. Technol.* **2021**, *55*, 9905–9915. [CrossRef]
12. Wang, Q.; Qi, J.; Wu, H.; Zeng, Y.; Shui, W.; Zeng, J.; Zhang, X. Freeze-Thaw cycle representation alters response of watershed hydrology to future climate change. *Catena* **2020**, *195*, 104767. [CrossRef]
13. Wang, Q.; Qi, J.; Li, J.; Cole, J.; Waldhoff, S.T.; Zhang, X. Nitrate loading projection is sensitive to freeze-thaw cycle representation. *Water Res.* **2020**, *186*, 116355. [CrossRef]
14. Wang, Q.; Zeng, J.; Leng, S.; Fan, B.; Tang, J.; Jiang, C.; Huang, Y.; Zhang, Q.; Qu, Y.; Wang, W.; et al. The effects of air temperature and precipitation on the net primary productivity in China during the early 21st century. *Front. Earth Sci.* **2018**, *12*, 818–833. [CrossRef]
15. Todisco, F.; Mannocchi, F.; Vergni, L. Severity–duration–frequency curves in the mitigation of drought impact: An agricultural case study. *Nat. Hazards* **2013**, *65*, 1863–1881. [CrossRef]
16. Giraldo Osorio, J.D.; Garcia Galiano, S.G. Non-stationary analysis of dry spells in monsoon season of Senegal River Basin using data from Regional Climate Models (RCMs). *J. Hydrol.* **2012**, *450*, 82–92. [CrossRef]
17. Masson-Delmotte, V.; Zhai, P.; Pirani, A.; Connors, S.L.; Péan, C.; Berger, S.; Caud, N.; Chen, Y.; Goldfarb, L.; Gomis, M.I. *Climate Change 2021: The Physical Science Basis: Contribution of Working Group I to the Sixth Assessment Report of the Intergovernmental Panel on Climate Change*; Cambridge University Press: Cambridge, UK, 2021; p. 2.
18. Zhang, A.; Jia, G. Monitoring meteorological drought in semiarid regions using multi-sensor microwave remote sensing data. *Remote Sens. Environ.* **2013**, *134*, 12–23. [CrossRef]
19. Burke, E.J.; Brown, S.J.; Christidis, N. Modeling the recent evolution of global drought and projections for the twenty-first century with the Hadley Centre climate model. *J. Hydrometeorol.* **2006**, *7*, 1113–1125. [CrossRef]
20. Zargar, A.; Sadiq, R.; Naser, B.; Khan, F.I. A review of drought indices. *Environ. Rev.* **2011**, *19*, 333–349. [CrossRef]
21. Palmer, W.C. *Meteorological Drought*; US Department of Commerce, Weather Bureau: Washington, DC, USA, 1965.
22. McKee, T.B.; Doesken, N.J.; Kleist, J. The relationship of drought frequency and duration to time scales. In Proceedings of the 8th Conference on Applied Climatology, Anaheim, CA, USA, 17–22 January 1993; Volume 17, pp. 179–183.
23. Vicente-Serrano, S.M.; Beguería, S.; López-Moreno, J.I. A Multiscalar Drought Index Sensitive to Global Warming: The Standardized Precipitation Evapotranspiration Index. *J. Clim.* **2010**, *23*, 1696–1718. [CrossRef]
24. Liu, Z.; Wang, Y.; Shao, M.; Jia, X.; Li, X. Spatiotemporal analysis of multiscalar drought characteristics across the Loess Plateau of China. *J. Hydrol.* **2016**, *534*, 281–299. [CrossRef]
25. Yu, M.; Li, Q.; Hayes, M.J.; Svoboda, M.D.; Heim, R.R. Are droughts becoming more frequent or severe in China based on the Standardized Precipitation Evapotranspiration Index: 1951–2010? *Int. J. Climatol.* **2014**, *34*, 545–558. [CrossRef]
26. Xu, X.; Piao, S.; Wang, X.; Chen, A.; Ciais, P.; Myneni, R.B. Spatio-temporal patterns of the area experiencing negative vegetation growth anomalies in China over the last three decades. *Environ. Res. Lett.* **2012**, *7*, 35701. [CrossRef]
27. Wang, L.; Chen, W. A CMIP5 multimodel projection of future temperature, precipitation, and climatological drought in China. *Int. J. Climatol.* **2014**, *34*, 2059–2078. [CrossRef]
28. Liu, M.; Xu, X.; Wang, D.; Sun, A.Y.; Wang, K. Karst catchments exhibited higher degradation stress from climate change than the non-karst catchments in southwest China: An ecohydrological perspective. *J. Hydrol.* **2016**, *535*, 173–180. [CrossRef]
29. Heilman, J.L.; Litvak, M.E.; McInnes, K.J.; Kjelgaard, J.F.; Kamps, R.H.; Schwinning, S. Water-storage capacity controls energy partitioning and water use in karst ecosystems on the Edwards Plateau, Texas. *Ecohydrology* **2014**, *7*, 127–138. [CrossRef]
30. Li, X.; He, B.; Quan, X.; Liao, Z.; Bai, X. Use of the Standardized Precipitation Evapotranspiration Index (SPEI) to Characterize the Drying Trend in Southwest China from 1982–2012. *Remote Sens.* **2015**, *7*, 10917–10937. [CrossRef]
31. Jia, Y.; Zhang, B.; Ma, B. Daily SPEI Reveals Long-term Change in Drought Characteristics in Southwest China. *Chin. Geogr. Sci.* **2018**, *28*, 680–693. [CrossRef]
32. Tang, H.; Wen, T.; Shi, P.; Qu, S.; Zhao, L.; Li, Q. Analysis of Characteristics of Hydrological and Meteorological Drought Evolution in Southwest China. *Water* **2021**, *13*, 1846. [CrossRef]

33. Zhang, L.; Xiao, J.; Li, J.; Wang, K.; Lei, L.; Guo, H. The 2010 spring drought reduced primary productivity in southwestern China. *Environ. Res. Lett.* **2012**, *7*, 45706. [CrossRef]
34. Nie, Y.; Chen, H.; Wang, K.; Yang, J. Water source utilization by woody plants growing on dolomite outcrops and nearby soils during dry seasons in karst region of Southwest China. *J. Hydrol.* **2012**, *420*, 264–274. [CrossRef]
35. Xu, K.; Yang, D.; Yang, H.; Li, Z.; Qin, Y.; Shen, Y. Spatio-temporal variation of drought in China during 1961–2012: A climatic perspective. *J. Hydrol.* **2015**, *526*, 253–264. [CrossRef]
36. Lloyd Hughes, B. A spatio-temporal structure-based approach to drought characterisation. *Int. J. Climatol.* **2012**, *32*, 406–418. [CrossRef]
37. Li, X.; Li, Y.; Chen, A.; Gao, M.; Slette, I.J.; Piao, S. The impact of the 2009/2010 drought on vegetation growth and terrestrial carbon balance in Southwest China. *Agric. For. Meteorol.* **2019**, *269–270*, 239–248. [CrossRef]
38. Wang, M.; Ding, Z.; Wu, C.; Song, L.; Ma, M.; Yu, P.; Lu, B.; Tang, X. Divergent responses of ecosystem water-use efficiency to extreme seasonal droughts in Southwest China. *Sci. Total Environ.* **2021**, *760*, 143427. [CrossRef] [PubMed]
39. Saft, M.; Western, A.W.; Zhang, L.; Peel, M.C.; Potter, N.J. The influence of multiyear drought on the annual rainfall-runoff relationship: An Australian perspective. *Water Resour. Res.* **2015**, *51*, 2444–2463. [CrossRef]
40. Yevjevich, V.M. *An Objective Approach to Definitions and Investigations of Continental Hydrologic Droughts*; Colorado State University Libraries: Fort Collins, CO, USA, 1967.
41. Mishra, A.K.; Singh, V.P. A review of drought concepts. *J. Hydrol.* **2010**, *391*, 204–216. [CrossRef]
42. Wu, R.; Zhang, J.; Bao, Y.; Guo, E. Run Theory and Copula-Based Drought Risk Analysis for Songnen Grassland in Northeastern China. *Sustainability* **2019**, *11*, 6032. [CrossRef]
43. Mesbahzadeh, T.; Mirakbari, M.; Saravi, M.M.; Sardoo, F.S.; Miglietta, M.M. Meteorological drought analysis using copula theory and drought indicators under climate change scenarios (RCP). *Meteorol. Appl.* **2020**, *27*, e1856. [CrossRef]
44. Liu, X.; Wang, S.; Zhou, Y.; Wang, F.; Li, W.; Liu, W. Regionalization and Spatiotemporal Variation of Drought in China Based on Standardized Precipitation Evapotranspiration Index (1961–2013). *Adv. Meteorol.* **2015**, *2015*, 950262. [CrossRef]
45. Da Rocha Junior, R.L.; Dos Santos Silva, F.D.; Costa, R.L.; Gomes, H.B.; Cavalcante Pinto, D.D.; Herdies, D.L. Bivariate Assessment of Drought Return Periods and Frequency in Brazilian Northeast Using Joint Distribution by Copula Method. *Geosciences* **2020**, *10*, 135. [CrossRef]
46. Caloiero, T.; Caroletti, G.N.; Coscarelli, R. IMERG-Based Meteorological Drought Analysis over Italy. *Climate* **2021**, *9*, 65. [CrossRef]
47. Mann, H.B. Nonparametric tests against trend. *Econom. J. Econom. Soc.* **1945**, *13*, 245–259. [CrossRef]
48. Zhang, H.; Zhang, Q.; Liu, X. Study on the main factors of aridity in Hetao area of North China. *Adv. Clim. Chang. Res.* **2016**, *12*, 20.
49. Xiong, G.; Zhang, B.; Li, C.; Shang, K.; Wang, S. Characteristics of drought variations in Southwest China in 1961–2012 based on SPEI. *Adv. Clim. Chang. Res.* **2013**, *9*, 192.
50. Huang, W.; Yang, X.; Li, M.; Zhang, X.; Wang, M.; Dai, S.; Ma, J. Evolution characteristics of seasonal drought in the south of China during the past 58 years based on standardized precipitation index. *Trans. Chin. Soc. Agric. Eng.* **2010**, *26*, 50–59.
51. Steinemann, A. Drought indicators and triggers: A stochastic approach to evaluation. *JAWRA J. Am. Water Resour. Assoc.* **2003**, *39*, 1217–1233. [CrossRef]
52. Yao, Y.; Liao, X.; Xiao, J.; He, Q.; Shi, W. The sensitivity of maize evapotranspiration to vapor pressure deficit and soil moisture with lagged effects under extreme drought in Southwest China. *Agric. Water Manag.* **2023**, *277*, 108101. [CrossRef]
53. Deng, Y.; Wang, X.; Wang, K.; Ciais, P.; Tang, S.; Jin, L.; Li, L.; Piao, S. Responses of vegetation greenness and carbon cycle to extreme droughts in China. *Agric. For. Meteorol.* **2021**, *298–299*, 108307. [CrossRef]
54. Li, Y.; Ren, F.; Li, Y.; Wang, P.; Yan, H. Characteristics of the regional meteorological drought events in Southwest China during 1960–2010. *J. Meteorol. Res.* **2014**, *28*, 381–392. [CrossRef]
55. Wang, L.; Chen, W. Characteristics of multi-timescale variabilities of the drought over last 100 years in Southwest China. *Adv. Meteorol. Sci. Technol.* **2012**, *2*, 21–26.
56. Cheng, Q.; Gao, L.; Zhong, F.; Zuo, X.; Ma, M. Spatiotemporal variations of drought in the Yunnan-Guizhou Plateau, southwest China, during 1960–2013 and their association with large-scale circulations and historical records. *Ecol. Indic.* **2020**, *112*, 106041. [CrossRef]
57. Zhang, C. Moisture sources for precipitation in Southwest China in summer and the changes during the extreme droughts of 2006 and 2011. *J. Hydrol.* **2020**, *591*, 125333. [CrossRef]
58. Sun, S.; Li, Q.; Li, J.; Wang, G.; Zhou, S.; Chai, R.; Hua, W.; Deng, P.; Wang, J.; Lou, W. Revisiting the evolution of the 2009–2011 meteorological drought over Southwest China. *J. Hydrol.* **2019**, *568*, 385–402. [CrossRef]
59. Lin, W.; Wen, C.; Wen, Z.; Gang, H. Drought in Southwest China: A review. *Atmos. Ocean. Sci. Lett.* **2015**, *8*, 339–344.
60. Liu, Y.; Ding, Z.; Chen, Y.; Yan, F.; Yu, P.; Man, W.; Liu, M.; Li, H.; Tang, X. Restored vegetation is more resistant to extreme drought events than natural vegetation in Southwest China. *Sci. Total Environ.* **2023**, *866*, 161250. [CrossRef] [PubMed]
61. Lu, J.; Ju, J.; Ren, J.; Gan, W. The influence of the Madden-Julian Oscillation activity anomalies on Yunnan's extreme drought of 2009–2010. *Sci. China-Earth Sci.* **2012**, *55*, 98–112. [CrossRef]
62. Qiu, J. China drought highlights future climate threats: Yunnan's worst drought for many years has been exacerbated by destruction of forest cover and a history of poor water management. *Nature* **2010**, *465*, 142–144. [CrossRef]

63. Zhao, X.; Wei, H.; Liang, S.; Zhou, T.; He, B.; Tang, B.; Wu, D. Responses of Natural Vegetation to Different Stages of Extreme Drought during 2009–2010 in Southwestern China. *Remote Sens.* **2015**, *7*, 14039–14054. [CrossRef]
64. Cui, L.; Zhang, C.; Yao, C.; Luo, Z.; Wang, X.; Li, Q. Analysis of the influencing factors of drought events based on GRACE data under different climatic conditions: A case study in Mainland China. *Water* **2021**, *13*, 2575. [CrossRef]
65. Wang, S.; Duan, H.; Feng, J. Drought events and its influence in autumn of 2010 in China. *J. Arid Meteorol.* **2010**, *32*, 1031–1039.
66. Wang, L.; Huang, G.; Chen, W.; Zhou, W.; Wang, W. Wet-to-dry shift over Southwest China in 1994 tied to the warming of tropical warm pool. *Clim. Dyn.* **2018**, *51*, 3111–3123. [CrossRef]
67. Thomas, T.; Jaiswal, R.K.; Nayak, P.C.; Ghosh, N.C. Comprehensive evaluation of the changing drought characteristics in Bundelkhand region of Central India. *Meteorol. Atmos. Phys.* **2015**, *127*, 163–182. [CrossRef]
68. Dai, A. Characteristics and trends in various forms of the Palmer Drought Severity Index during 1900–2008. *J. Geophys. Res. Atmos.* **2011**, *116*, D12115. [CrossRef]
69. Liu, B.; Chen, C.; Lian, Y.; Chen, J.; Chen, X. Long-term change of wet and dry climatic conditions in the southwest karst area of China. *Glob. Planet. Chang.* **2015**, *127*, 1–11. [CrossRef]
70. Han, L.Y.; Zhang, Q.; Yao, Y.B.; Li, Y.; Jia, J.; Wang, J. Characteristics and origins of drought disasters in Southwest China in nearly 60 years. *Acta Geogr. Sin.* **2014**, *69*, 632–639.
71. Su, X.C.; Wang, L.; Li, Q.L.; Teng, C. Study of surface dry and wet conditions in Southwest China in recent 50 years. *J. Nat. Resour.* **2014**, *29*, 104–116.
72. Wang, D.; Zhang, B.; An, M.; Zhang, T.; Ji, D.; Ren, P. Temporal and spatial distributions of drought in Southwest China over the past 53 years based on standardized precipitation evapotranspiration index. *J. Nat. Resour.* **2014**, *29*, 1003–1016.
73. Mei, S.; Chen, S.; Li, Y.; Aru, H. Interannual Variations of Rainfall in Late Spring over Southwest China and Associated Sea Surface Temperature and Atmospheric Circulation Anomalies. *Atmosphere* **2022**, *13*, 735. [CrossRef]
74. Li, G.; Li, C.; Zhou, W.; Wen, B. Climatic characteristics of rainfall over Southwest China during spring and spring months. *Clim. Environ. Res.* **2020**, *25*, 575–587.
75. Brown, J.F.; Wardlow, B.D.; Tadesse, T.; Hayes, M.J.; Reed, B.C. The Vegetation Drought Response Index (VegDRI): A new integrated approach for monitoring drought stress in vegetation. *Gisci. Remote Sens.* **2008**, *45*, 16–46. [CrossRef]
76. Quiring, S.M. Developing objective operational definitions for monitoring drought. *J. Appl. Meteorol. Climatol.* **2009**, *48*, 1217–1229. [CrossRef]
77. Ines, A.V.; Das, N.N.; Hansen, J.W.; Njoku, E.G. Assimilation of remotely sensed soil moisture and vegetation with a crop simulation model for maize yield prediction. *Remote Sens. Environ.* **2013**, *138*, 149–164. [CrossRef]
78. Mladenova, I.E.; Bolten, J.D.; Crow, W.T.; Anderson, M.C.; Hain, C.R.; Johnson, D.M.; Mueller, R. Intercomparison of soil moisture, evaporative stress, and vegetation indices for estimating corn and soybean yields over the US. *IEEE J. Sel. Top. Appl. Earth Obs. Remote Sens.* **2017**, *10*, 1328–1343. [CrossRef]
79. Afshar, M.H.; Bulut, B.; Duzenli, E.; Amjad, M.; Yilmaz, M.T. Global spatiotemporal consistency between meteorological and soil moisture drought indices. *Agric. For. Meteorol.* **2022**, *316*, 108848. [CrossRef]
80. Bergman, K.H.; Sabol, P.; Miskus, D. Experimental indices for monitoring global drought conditions. In Proceedings of the 13th Annual Climate Diagnostics Workshop, Cambridge, MA, USA, 31 October–4 November 1988; Volume 31, pp. 190–197.
81. Dutra, E.; Viterbo, P.; Miranda, P.M. ERA-40 reanalysis hydrological applications in the characterization of regional drought. *Geophys. Res. Lett.* **2008**, *35*, L19402. [CrossRef]
82. Sridhar, V.; Hubbard, K.G.; You, J.; Hunt, E.D. Development of the soil moisture index to quantify agricultural drought and its "user friendliness" in severity-area-duration assessment. *J. Hydrometeorol.* **2008**, *9*, 660–676. [CrossRef]
83. Martínez-Fernández, J.; González-Zamora, A.; Sánchez, N.; Gumuzzio, A. A soil water based index as a suitable agricultural drought indicator. *J. Hydrol.* **2015**, *522*, 265–273. [CrossRef]
84. Bulut, B.; Yilmaz, M.T.; Afshar, M.H.; Şorman, A.Ü.; Yücel, İ.; Cosh, M.H.; Şimşek, O. Evaluation of remotely-sensed and model-based soil moisture products according to different soil type, vegetation cover and climate regime using station-based observations over Turkey. *Remote Sens.* **2019**, *11*, 1875. [CrossRef]
85. Li, Q.; Shi, G.; Shangguan, W.; Nourani, V.; Li, J.; Li, L.; Huang, F.; Zhang, Y.; Wang, C.; Wang, D.; et al. A 1 km daily soil moisture dataset over China using in situ measurement and machine learning. *Earth Syst. Sci. Data* **2022**, *14*, 5267–5286. [CrossRef]